

Research Article

Open Access

Virendra Kumar Chaudhari, Niranjana L. Shegokar, and Achchhe Lal*

Nonlinear free vibration analysis of elastically supported carbon nanotube-reinforced composite beam with the thermal environment in non-deterministic framework

DOI 10.1515/cls-2017-0007

Received Oct 11, 2016; accepted Nov 24, 2016

Abstract: This paper deals with the investigation of nonlinear free vibration behavior of elastically supported carbon nanotube reinforced composite (CNTRC) beam subjected to thermal loading with random system properties. Material properties of each constituent's material, volume fraction exponent and foundation parameters are considered as uncorrelated Gaussian random input variables. The beam is supported by a Pasternak foundation with Winkler cubic nonlinearity. The higher order shear deformation theory (HSDT) with von-Karman nonlinearity is used to formulate the governing equation using Hamilton principle. Convergence and validation study is carried out through the comparison with the available results in the literature for authenticity and accuracy of the present approach used in the analysis. First order perturbation technique (FOPT), Second order perturbation technique (SOPT) and Monte Carlo simulation (MCS) methods are employed to investigate the effect of geometric configuration, volume fraction exponent, foundation parameters, distribution of reinforcement and thermal loading on nonlinear vibration characteristics CNTRC beam. The present work signifies the accurate analysis of vibrational behaviour influences by different random variables. Results are presented in terms of mean, variance (COV) and probability density function (PDF) for various aforementioned parameters.

Keywords: Carbon nanotube-reinforced composite beam; nonlinear free vibration; elastic foundation; Probability density function; Variance; Random system properties; FOPT; SOPT; MCS

1 Introduction

Carbon nanotubes (CNTs), a new high technological advanced material of extraordinary strength and stiffness with high aspect ratio and low density, have seized considerable attention of researchers since last several decades, Iijima [1]. Motivated by their extraordinary mechanical properties, carbon nanotubes (CNTs) have great potential for being used for reinforcement of high strength and light-weight polymer composites, Thostenson *et al.* [2], Lau *et al.* [3]. Many researchers have paid much attention on the mechanical properties of carbon nanotube-reinforced composites (CNTRC), Wuite and Adali [4], Vodenitcharova and Zhang [5]. Hu *et al.* [6] evaluated the macroscopic elastic properties of CNTRC by analyzing the elastic deformation of a representative volume element under several loading conditions. Using molecular dynamics (MD), Han and Elliott [7] simulated the elastic properties of polymer/carbon nanotube composites. Wan *et al.* [8] investigated the effective moduli of the CNT reinforced polymer composite, with emphasis on the influence of CNT length and CNT matrix inter phase on the stiffening of the composite.

The study of the vibration characteristics of the structure resting on elastic foundation is an important concern while designing resonant-free structural components. It is noteworthy that during the vibration analysis of such type of beam, uncertainty in the foundation parameters and material non-linearity cannot be avoided in a real time manner.

A considerable spectrum of literature is available on the linear and nonlinear free vibration response of geometrically nonlinear composite panels such as beam, plate and shells supported by and without foundation subjected to thermo mechanical loadings using deterministic system

*Corresponding Author: Achchhe Lal: S.V. National Institute of Technology, Surat - 395007, India;
Email: achchhelal@med.svnit.ac.in

Virendra Kumar Chaudhari: Dr. D C National polytechnic, Sidhartha Nagar, U.P - 272153, India

Niranjana L. Shegokar: Dr D Y Patil School of Engineering & Technology, Lohegaon, Pune- 41210, India

properties. In the same direction, Shooshtari and Rafiee [9] presented the nonlinear forced vibration response of functionally graded based on Euler-Bernoulli beam theory and von Karman geometric nonlinearity. Yang and Chen [10] investigated free vibration and buckling analysis of FGM beam with open crack at their edge by using Bernoulli-Euler beam theory and the rotation spring model. Liao-Liang Ke *et al.* [11] investigated the nonlinear free vibration of functionally graded nanocomposite beams reinforced by single-walled carbon nanotubes (SWCNTs) based on Timoshenko beam theory.

Kitipornchai *et al.* [12] derived the eigenvalue equation by using Ritz method via direct iterative method to generate the nonlinear forced vibration of a cracked FGM beam with different end supports based von Karman geometric nonlinearity. Sina *et al.* [13] formulated the analytical solution for a free vibration of FGMs beam using first order shear deformation theory (FSDT). Aydogdu [14] used various higher order shear deformation theories and classical beam theories to obtain free vibration frequencies and mode shapes for different material properties and slenderness ratios. Shen and Xiang [15] studied the behaviors of large amplitude vibration, nonlinear bending and thermal post buckling of elastically supported nanocomposite beams reinforced by SWCNTs in thermal environments. S. Boutaleb *et al.* [16] proposed a micromechanical analytical model for the problem of stiffness and yield stress prediction in the case of nanocomposite consisting of silica nanoparticles embedded in a polymer matrix.

Devalve and Pitchumani [17] presented a numerical model to describe the vibration damping effects of CNTs embedded in the matrix of fiber-reinforced composite materials used in rotating structures. KE *et al.* [18] presented a dynamic stability analysis of functionally graded nanocomposite beams reinforced by SWCNTs based on Timoshenko beam theory. Yas and Samadi [19] investigated stability and dynamic analysis of nanocomposite Timoshenko beams reinforced by SWCNTs resting on an elastic foundation and governing equations are derived through using Hamilton's principle and then solved by using the generalized differential quadrature method (GDQM). Rao and Varma [20] presented thermal post buckling and large-amplitude vibration formulations of beams. Mehdipour *et al.* [21] investigated the effects of the curvature or waviness and midplane stretching of the nanotube on the nonlinear frequency by utilizing He's Energy Balance Method (HEBM).

However, a few literatures are available on the linear and nonlinear vibration of CNTRCs and composite structures resting on elastic foundation. Lee and Chang [22] analyzed the vibration of fluid-filled SWCNTs embedded in an

elastic medium by using the Winkler - type model. Pradhan and Murmu [23] used nonlocal beam theory and Winkler foundation model for vibration analysis of beam surrounded by elastic medium. Murmu and Pradhan [24] used nonlocal elasticity theory to study of thermo-mechanical vibration of a SWCNT embedded in an elastic medium. Yoon *et al.* [25] used the multiple-elastic beam model for the vibration analysis of multiwall carbon nanotubes surrounded in an elastic medium. These works were based on nonlocal Euler-Bernoulli beam model. The Timoshenko beam theory considers the shear deformation and the rotary inertia effect into account, is more accurate than the Euler-Bernoulli beam theory, Timoshenko *et al.* [26]. Chaudhari and Lal [27] investigated the nonlinear behavior of shear deformable CNTRC beam using finite element method. Fantuzzi *et al.* [28] investigated the agglomeration behavior of the reinforcing phase for fluctuating values of the parameters that control both the density of CNTs within the spherical inclusions, and the quantities of nanofibers scattered in the polymeric matrix. Tornabene *et al.* [29] studied the linear static response of nanoplates and nanoshells are considerably affected by the agglomeration of CNT.

The above mentioned literatures are based on deterministic analysis. In the deterministic analysis, the mean value of material properties gives only mean response and unaccounted deviation caused due to inherent material properties. However, the studies related to stochastic analyses are limited. Certain effort have been made in the past by the researchers to predict the structural response of structures with random system properties.

In this direction, Shegokar and Lal [30] investigated second order statistics of large amplitude free flexural vibration of shear deformable functionally graded materials (FGMs) beams with surface-bonded piezoelectric layers subjected to thermo piezoelectric loadings with random material properties. Vanmarcke and Grigoriu [31] evaluated the second order statistics of deflection behavior of beam using random material properties and rigidity via correlation method. Kaminski [32] evaluated bending response using second order perturbation and second order probabilistic moment method via stress-based finite element method. Locke [33] presented the thermally buckled and vibration analysis for large deflection response using iterative techniques and method of linearization. Onkar *et al.* [34] presented the generalized force nonlinear vibration of laminated composite plate with random material properties using classical plate theory (CLT) combined with FOPT. Kitipornchai *et al.* [35] studied the vibration composed by the third order shear deformation theory with random material effect using FOPT incorporating mixed

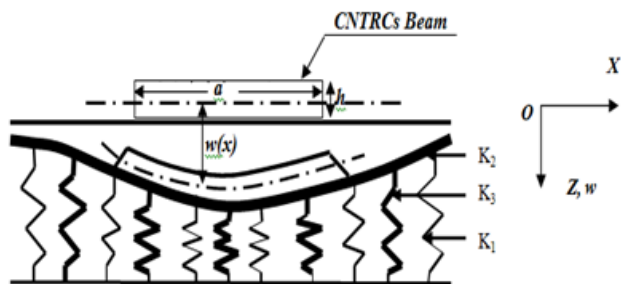


Figure 1: Geometry of CNTRC beam resting on nonlinear elastic foundation.

type and semi analytical approach to derive the standard eigenvalue problem.

Shaker *et al.* [36] presented the stochastic finite element method (SFEM) to investigate the natural frequency of composite laminated and functionally graded plates HSDT based on first order reliability method and second order reliability method. Lal *et al.* [37, 38] evaluated the linear and nonlinear free vibration response of laminated composite plates with and without resting on elastic foundation and thermal environment using HSDT. Jagtap *et al.* [39] examined the stochastic nonlinear free vibration response of FGM plate using HSDT with von-Karman kinematic nonlinear via direct iterative based stochastic finite element method.

It is evident from the literature that limited literature is reported on the laminated composite structures with uncertain system properties. However, a very few studies are available on the linear and nonlinear vibration analysis of the composite plates with random material properties with or without elastic foundation. The literature reveals that no attempt has been made to study the nonlinear free vibration response of uncertain CNTRC beam resting on nonlinear elastic foundations using SOPT and MCS in the framework of the HSDT with von-Karman nonlinearity, to the best of the authors' knowledge.

In the present study, both material thermo mechanical properties of CNTRC, matrix and foundation parameters are treated as normal Gaussian uncorrelated random variables in a stochastic finite element method by SOPT with taking advantageous of MCS for predicting the natural frequency of CNTRC elastically supported beam. The effect of geometric configuration, volume fraction exponent, foundation parameters, distribution of reinforcement and thermal loading on nonlinear vibration characteristics CNTRC beam is investigated. Results are shown in terms of mean, variance (COV) and probability density function (PDF) for various aforementioned parameters.

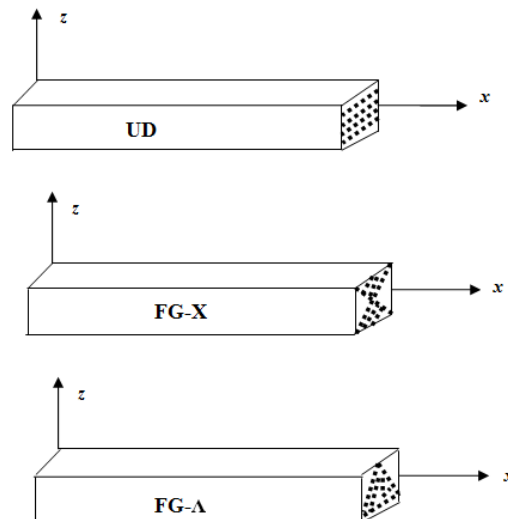


Figure 2: Configurations of the CNTRC in composite beams.

2 Formulations

2.1 Geometric configuration

Consider a CNTRC beam supported by nonlinear elastic foundation consist of linear and nonlinear spring and shear foundation of length a and thickness h located in one dimensional plane with its coordinate definition and material directions of typical lamina in (x, z) coordinate system as shown in Fig. 1. The CNTRC beam is assumed to be attached to the foundation which is not separable during the process of deformation. The interaction between the beam and the supporting foundation follows the two parameters model (Pasternak-type) with Winkler cubic nonlinearity as [37, 38].

$$p = K_1 w + K_2 w^3 + K_3 \nabla w \quad (1)$$

Where p and w are the foundation reaction per unit area and transverse displacement, respectively, the parameters ∇ , K_1 , K_2 and K_3 are Laplace differential operator, linear normal, shear and nonlinear normal stiffnesses of the foundation, respectively.

2.2 Material properties of CNTRC beams

The distribution of CNTs is considered in the depth of the composite beams as shown in Fig. 2. In this figure the density of CNTs within the area is constant and the volume fraction of CNTs varies through the depth of the beam and uniform distribution (UD) and functionally graded distributions (FG-A, and FG-X) are shown. In the present analysis an embedded carbon nanotube in a polymer matrix is

used. It is assumed the CNTRC beams are made of a mixture of SWCNTs and an isotropic matrix and no abrupt interface between the CNT and polymer matrix in the entire region of the beam. To evaluate the effective material properties of CNTRC, rule of mixture [7, 8], and [15] is employed. According to rule of mixture model, the effective Young's moduli and shear modulus of CNTRC beams can be expressed as

$$E_{11} = \eta_1 V_{cn} E_{11}^{cn} + V_m E^m \quad (2)$$

$$\frac{\eta_2}{E_{22}} = \frac{V_{cn}}{E_{22}^{cn}} + \frac{V_m}{E^m} \quad (3)$$

$$\frac{\eta_3}{G_{12}} = \frac{V_{cn}}{G_{12}^{cn}} + \frac{V_m}{E^m} \quad (4)$$

where E_{11}^{cn} , E_{12}^{cn} , G_{12}^{cn} , E_m and G_m are the Young's moduli and shear modulus of the SWCNTs and matrix, respectively. It has been stated that the load transfer between the nanotube and polymeric phases is less than perfect due to surface effects, strain gradients effects, and intermolecular coupled stress effects, hence, the efficiency parameters η_j ($j = 1, 2, 3$) in Eqs (2–4) is considered. Efficiency parameters will be intended later by matching the elastic moduli of CNTRCs predicted by the MD simulations with the numerical results obtained from the rule of mixture. In addition, V_{cn} and V_m are the volume fraction of the carbon nanotube (CNT) and the matrix which fulfill the relationship of $V_{cn} + V_m = 1$.

Similarly, Poisson's ratio ν and mass density ρ of the CNTRC beams can be expressed as:

$$\nu = V_{cn} \nu^{cn} + V_m \nu^m, \quad \rho = V_{cn} \rho^{cn} + V_m \rho^m \quad (5)$$

Where ν^{cn} , ν^m , ρ^{cn} , and ρ^m are the Poisson's ratios and densities of CNT and matrix, respectively.

The different distributions of the CNTs in the CNTRCs beams depicted in Fig. 2 are assumed to be as follows:

$$\text{UD case: } V_{cn} = V_{cn}^* \quad (6)$$

$$\text{FG-Acase: } V_{cn} = 2 \left(1 + \frac{2z}{h} \right) V_{cn}^* \quad (7)$$

$$\text{FG-Xcase: } V_{cn} = 2 - 4 \frac{|z|}{h} V_{cn}^* \quad (8)$$

where V_{cn}^* is the volume fraction of CNTs and can be evaluated as

$$V_{cn} = \frac{W_{cn}}{W_{cn} + \left(\frac{\rho^{cn}}{\rho^m} \right) - \left(\frac{\rho^{cn}}{\rho^m} \right) W_{cn}} \quad (9)$$

Similarly, the effective thermal expansion coefficients in the longitudinal and transverse directions (α_{11} , α_{22}) graded in the z direction can be expressed as

$$\alpha_{11} = \frac{V_{cn} E_{11}^{cn} \alpha_{11}^{cn} + V_m E^m \alpha^m}{V_{cn} E_{11}^{cn} + V_m E^m} \quad (10)$$

$$\alpha_{22} = (1 + \nu_{12}^{cn}) V_{cn} \alpha_{22}^{cn} + (1 + \nu^m) V_m \alpha^m - \nu_{12} \alpha_{11} \quad (11)$$

It is assumed that the material properties of CNTs and matrix are the functions of temperature, so that the effective material properties of FG-CNTRCs, like Young's modulus, shear modulus and thermal expansion coefficients, are also functions of temperature T and position z .

2.3 Displacement field model

For an arbitrary CNTRC beam, the components of the displacement field model can be expressed as the modified displacement field components along x and z directions of an arbitrary point within the beam based on the HSDT using C^0 continuity can be expressed as Chaudhari and Lal [27]

$$\bar{u}(x, z) = u + f_1(z) \psi_x + f_2(z) \phi_x; \quad \bar{w}(x, z) = w \quad (12)$$

Where u , w , Ψ_x and $\phi = \frac{\partial w}{\partial x}$ are the mid-plane axial displacement, transverse displacement, rotation of normal to the mid-plane along y -axis and slope along x -axis, respectively

$$\text{Where } f_1(z) = C_1 z - C_2 z^3, \quad f_2(z) = -C_4 z^3, \quad (13)$$

$$\text{With } C_1 = 1, \quad C_2 = C_4 = 4/3h^2$$

The displacement vector for the modified C^0 continuous model can be written as

$$\{q\} = \left[u \quad w \quad \theta_x \quad \psi_x \right]^T \quad (14)$$

2.4 Strain displacement relation

The total strain vector consisting of linear strain (in terms of mid plane deformation, rotation of normal and higher order terms), non-linear strain (von-Karman type), thermal strains vectors associate with the displacement for CNTRC beam can be expressed as

$$\{\bar{\epsilon}\} = \{\bar{\epsilon}^L\} + \{\bar{\epsilon}^{NL}\} - \{\bar{\epsilon}^T\} \quad (15)$$

where $\{\bar{\epsilon}^L\}$, $\{\bar{\epsilon}^{NL}\}$ and $\{\bar{\epsilon}^T\}$ are the linear, non-linear and thermal strain vectors, respectively.

From Eq. (15), the linear strain tensor using HSDT can be written as

$$\bar{\varepsilon}^L = [B]\{q\} \quad (16)$$

where $[B]$ and $\{q\}$ are the geometrical matrix and displacement field vector, respectively.

The nonlinear strain vector $\{\bar{\varepsilon}^{NL}\}$ can be written as

$$\bar{\varepsilon}^{NL} = \frac{1}{2} [A_{nl}] \{\phi_{nl}\} \quad \text{Where } \{A_{nl}\} = \frac{1}{2} \left[\frac{\partial w}{\partial x} \right]^T \quad (17)$$

and $\{\phi_{nl}\} = \left\{ \frac{\partial w}{\partial x} \right\}$

The thermal strain vector $\{\bar{\varepsilon}^T\}$ induced by uniform and non-uniform temperature change can be expressed as

$$\{\bar{\varepsilon}^T\} = \{\alpha_x\} \Delta T \quad (18)$$

Where $\{\alpha_x\}$ is coefficients of thermal expansion along the x direction, and ΔT is the change in temperature in the CNTRC beam considered as uniform and non-uniform type.

The uniform change in temperature (ΔT) can be expressed as

$$\Delta T = T - T_0 \quad (19)$$

Where, T is the uniform temperature rise and T_0 is the room temperature and assumed as 300K.

2.5 Stress- Strain relation

The relation between stress and strain for the plane-stress case using thermo-elastic constitutive relation can be written as

$$\{\bar{\sigma}\} = [Q] \{\bar{\varepsilon}\} \quad (20)$$

$$\begin{Bmatrix} \bar{\sigma}_x \\ \bar{\tau}_{xz} \end{Bmatrix} = \begin{bmatrix} Q_{11} & 0 \\ 0 & Q_{55} \end{bmatrix} \left\{ \left\{ \bar{\varepsilon}^L \right\} + \left\{ \bar{\varepsilon}^{NL} \right\} - \left\{ \bar{\varepsilon}^T \right\} \right\} \quad (21)$$

where

$$Q_{11}(z) = \frac{E_z}{1 - \nu^2(z)}, \quad Q_{55}(z) = G_{12}(z) \quad (22)$$

2.6 Strain energy of CNTRC beam

The strain energy (Π_1) of the CNTRC beam undergoing large deformation can be expressed as

$$\Pi_1 = U_L + U_{NL} \quad (23)$$

The linear strain energy (U_L) of the CNTRC beam is given by

$$\begin{aligned} U_L &= \int_A \frac{1}{2} \left\{ \bar{\varepsilon}^L \right\}^T [Q] \left\{ \bar{\varepsilon}^L \right\} dA \quad (24) \\ &= \int_A \frac{1}{2} \left\{ \bar{\varepsilon}^L \right\}^T [D] \left\{ \bar{\varepsilon}^L \right\} dA \end{aligned}$$

where $[D]$ and $\{\bar{\varepsilon}^L\}$ are the elastic stiffness matrix and linear strain vector, respectively.

The nonlinear strain energy (U_{NL}) of the CNTRC beam can be rewritten as

$$\begin{aligned} U_{NL} &= \int_A \frac{1}{2} \left\{ \bar{\varepsilon}^L \right\} [D_1] \left\{ \bar{\varepsilon}^{NL} \right\}^T dA \quad (25) \\ &+ \frac{1}{2} \int_A \left\{ \bar{\varepsilon}^{NL} \right\} [D_2] \left\{ \bar{\varepsilon}^L \right\}^T dA \\ &+ \frac{1}{2} \int_A \left\{ \bar{\varepsilon}^{NL} \right\} [D_3] \left\{ \bar{\varepsilon}^{NL} \right\}^T dA \end{aligned}$$

where D_1 , D_2 and D_3 are the elastic stiffness matrices of the CNTRC beam, respectively.

2.7 Strain energy due to foundation

The strain energy due to elastic foundation having a shear deformable layer with Winkler cubic nonlinearity is expressed as

$$U_F = \frac{1}{2} \int_V p w dV \quad (26)$$

The strain energy due to the foundation is expressed as

$$U_F = \frac{1}{2} \int_A \left\{ K_1 w^2 + \frac{1}{2} K_3 w^4 + K_2 \left[(w_{,x})^2 + (w_{,x})^2 \right] \right\} dA \quad (27)$$

$$\begin{aligned} U_F &= \frac{1}{2} \int_A \begin{Bmatrix} w \\ w_{,x} \end{Bmatrix}^T \begin{bmatrix} K_1 & 0 \\ 0 & K_2 \end{bmatrix} \begin{Bmatrix} w \\ w_{,x} \end{Bmatrix} dA \quad (28) \\ &+ \frac{1}{2} \int_A \begin{Bmatrix} w \\ w_{,x} \end{Bmatrix}^T \begin{bmatrix} K_3 w^2 & 0 \\ 0 & 0 \end{bmatrix} \begin{Bmatrix} w \\ w_{,x} \end{Bmatrix} dA \end{aligned}$$

2.8 Work done due to thermal loadings

The potential of work (Π_2) storage due to thermal loadings can be written as

$$\Pi_2 = \frac{1}{2} \int_A N_0^T (w_{,x})^2 dA \quad (29)$$

The thermal compressive stress/unit length N_0^T can be expressed as

$$N_0^T = \begin{bmatrix} N_x^T & M_x^T & P_x^T \end{bmatrix} \quad (30)$$

The Eq. (31) can be further written as

$$N_0^T = \int_{-h/2}^{h/2} (1, z, z^3)(Q_{11})\alpha\Delta T dz \quad (31)$$

2.9 Kinetic energy of the CNTRC beam

The kinetic energy (T) of the vibrating FGM beam can be expressed as [27, 36, 37]

$$T = \frac{1}{2} \int_v \rho \hat{u}^T \hat{u} dv \quad (32)$$

where ρ and $\{\hat{u}\}$ are the density and velocity vector of the FGM beam, respectively.

$$\begin{aligned} T &= \frac{1}{2} \int_0^l \int_{-h/2}^{h/2} \rho(z) \left[(\bar{u})^2 + (\bar{w})^2 \right] dz dx \quad (33) \\ &= \frac{1}{2} \int_0^l \int_{-h/2}^{h/2} \rho(z) N^T N dz dx \end{aligned}$$

3 Finite Element Model

3.1 Strain energy of the beam element

The present study includes a C^0 one-dimensional Hermitian beam element having 4 DOFs each node. Chaudhari and Lal [27] expressed as this type of beam element geometry and the displacement vector.

$$\{q\} = \sum_{i=1}^{NN} N_i \{q\}_i; \quad x = \sum_{i=1}^{NN} N_i x_i; \quad (34)$$

N_i and $\{q\}_i$ signify the interpolation function for the i th node and the vector of unknown displacements for the i th node, correspondingly. The parameter NN shows the number of nodes per element and x_i shows the Cartesian coordinate. The axial displacement and rotation of normal are represented by linear interpolation function and while, for transverse displacement and slope by Hermite cubic interpolation functions.

Using finite element model Eq. (34), Eq. (23) can be expressed as

$$\prod = \sum_{e=1}^{NE} \prod_a^{(e)} = \sum_{e=1}^{NE} \left(U_L^{(e)} + U_{NL}^{(e)} \right) \quad (35)$$

Where, NE and (e) denote the number of elements and element, respectively.

Substituting Eq. (24) and Eq. (25) into Eq. (35), Eq. (35) can be further expressed as

$$\begin{aligned} \Pi_1 &= \frac{1}{2} \sum_{e=1}^{NE} \left[\{q\}^{T(e)} [K_l + K_{nl}]^{(e)} \{q\}^{(e)} \right] \quad (36) \\ &= \{q\}^T [K_l + K_{nl}] \{q\} \end{aligned}$$

Here $[K_{nl}] = \frac{1}{2} [K_{nl_1}] + [K_{nl_2}] + \frac{1}{2} [K_{nl_3}]$

Where, $[K_l]$, $[K_{nl_1}]$, $[K_{nl_2}]$, $[K_{nl_3}]$ and $\{q\}$ are defined as global linear, nonlinear stiffness matrices and global displacement vector, respectively.

Similarly, using finite element model Eq. (34), Eq. (27) after the assembly procedure can be written as

$$\begin{aligned} \Pi_F &= \sum_{e=1}^{NE} \left(\Pi_F^{(e)} \right) = \left\{ \Delta^{(e)} \right\} [K_{fl} + K_{fml}(\Delta)]^{(e)} \left\{ \Delta^{(e)} \right\} \quad (37) \\ &= \{q\} [K_{fl} + K_{fml}(q)] \{q\} \end{aligned}$$

where, $[K_{fl}]$ and $[K_{fml}(q)]$ is the global linear and nonlinear foundation stiffness matrices, respectively.

Using finite element model Eq. (34), Eq. (29) after summing over the entire element can be written as

$$\begin{aligned} \Pi_2 &= \sum_{e=1}^{NE} \Pi_2^{(e)} = \frac{1}{2} \sum_{e=1}^{NE} \{q\}^{T(e)} \lambda [K_g]^{(e)} \{q\}^{(e)} \quad (38) \\ &= \frac{1}{2} \lambda \{q\}^T [K_g] \{q\} \end{aligned}$$

where, λ and $[K_g]$ are defined as the thermal buckling load parameters and the global geometric stiffness matrix, respectively.

Using finite element model as given in Eq. (34), Eq. (33) may be written as

$$T = \sum_{e=1}^{NE} \left\{ \Lambda \right\}^{(e)T} [m] \left\{ \Lambda \right\}^{(e)} = \left\{ q \right\}^T [M] \left\{ q \right\} \quad (39)$$

where, $[M]$ is the global consistent mass matrix [27].

4 Governing equation

The governing equation for the nonlinear static analysis can be derived using Lagrange equation for a conservative system and can be written as [27].

$$\frac{d}{dt} \left(\frac{\partial T}{\partial \dot{q}} \right) + \frac{\partial \Pi_1}{\partial q} + \frac{\partial \Pi_f}{\partial q} - \frac{\partial \Pi_2}{\partial q} = 0 \quad (40)$$

By substituting the Eq. (36–39), in Eq. (40) and simplification gives us

$$M\ddot{q} + Kq = 0 \quad (41)$$

where $[K] = \{[K_l] + [K_{nl}] + [K_{lf}] + [K_{nlf}] - [K_G]\}$

The above Eq. (41) is the nonlinear free vibration equation that can be solved iteratively as a linear eigenvalue problem, assuming that the beam is vibrating in its principal mode in each iteration. For each iteration, Eq. (41) can be expressed as a generalized eigenvalue problem as [27]:

$$[K] \{q\} = \lambda [M] \{q\} \quad (42)$$

The stiffness matrix $[K]$ consists of linear and nonlinear stiffness matrix, foundation matrix and geometric stiffness matrix $[K_G]$, mass matrix $[M]$, and displacement vector $\{q\}$ are random in nature, being dependent on the system properties of the structure. Consequently, the nonlinear natural frequency (ω_{nl}) and its mode shape are random in nature. Therefore the eigenvalue and eigenvectors also become random. In deterministic environment, the solution of Eq. (42) can be obtained using standard solution procedure such as direct iterative, incremental and/or Newton-Raphson method etc. However, in random environment to obtain the complete solution of Eq. (42), statistical analysis through SOPT and MCS methods combined with direct iterative analysis is required.

5 Solution approach

5.1 A Direct iterative method for nonlinear vibration problem

The nonlinear eigenvalue problem as given in Eq. (42) is assuming that the random changes in eigenvector during iterations does not affect much the nonlinear stiffness matrix and solved by implementing probabilistic approaches [37, 38].

5.2 Stochastic solution approach

In the present non-deterministic analysis, finite element based on FOPT, SOPT and MCS methods are adopted to quantify the structural response uncertainties by making explicit treatment of uncertainties in any or combined quantities. The existing uncertain variations in parameters may have significant effects on the fundamental structural characteristic in the form of nonlinear free vibration; consequently, this uncertain parameter must affect the final design. The FOPT and SOPT based on Taylor series expansion is used to formulate the linear relationship between some characteristics of the random response and random structural constraints on the basis of perturbation

tactic. However, the applicability of these methods is limited due to valid for small coefficient of variation (COV) of input random variables [37, 38]. The descriptions of these methods are given as follows.

In this method, the stiffness matrix K , mass matrix M and displacement vector q ; are expanded in terms of the random variable α_i which represent the structural uncertainty existing in the CNTRC elastically supported beam, as follows:

$$[K] = [K^{(0)}] + \sum_{i=1}^N [K_i^{(1)}] \alpha_i + \frac{1}{2} \sum_{i=1}^N \sum_{j=1}^N [K_{ij}^{(2)}] \alpha_i \alpha_j \quad (43)$$

$$[q] = [q^{(0)}] + \sum_{i=1}^N [q_i^{(1)}] \alpha_i + \frac{1}{2} \sum_{i=1}^N \sum_{j=1}^N [q_{ij}^{(2)}] \alpha_i \alpha_j$$

$$[\lambda] = [\lambda^{(0)}] + \sum_{i=1}^N [\lambda_i^{(1)}] \alpha_i + \frac{1}{2} \sum_{i=1}^N \sum_{j=1}^N [\lambda_{ij}^{(2)}] \alpha_i \alpha_j$$

$$[M] = [M^{(0)}] + \sum_{i=1}^N [M_i^{(1)}] \alpha_i + \frac{1}{2} \sum_{i=1}^N \sum_{j=1}^N [M_{ij}^{(2)}] \alpha_i \alpha_j$$

where $\alpha_i = \alpha_0 - \alpha_i$ with α_0 denoting the mean value of random variable α_i , $K^{(0)}$, $M^{(0)}$, and $q^{(0)}$ is the zeroth order of stiffness matrix, mass matrix and eigenvector which are identical to deterministic values, $K_i^{(1)} = \left. \frac{\partial K}{\partial \alpha_i} \right|_{\alpha=0}$, $K_{ij}^{(2)} = \left. \frac{\partial^2 K}{\partial \alpha_i \partial \alpha_j} \right|_{\alpha=0}$, $q_i^{(1)} = \left. \frac{\partial q}{\partial \alpha_i} \right|_{\alpha=0}$, $q_{ij}^{(2)} = \left. \frac{\partial^2 q}{\partial \alpha_i \partial \alpha_j} \right|_{\alpha=0}$, $\lambda_i^{(1)} = \left. \frac{\partial \lambda}{\partial \alpha_i} \right|_{\alpha=0}$, $\lambda_{ij}^{(2)} = \left. \frac{\partial^2 \lambda}{\partial \alpha_i \partial \alpha_j} \right|_{\alpha=0}$, $M_i^{(1)} = \left. \frac{\partial M}{\partial \alpha_i} \right|_{\alpha=0}$, and $M_{ij}^{(2)} = \left. \frac{\partial^2 M}{\partial \alpha_i \partial \alpha_j} \right|_{\alpha=0}$, and are the first and second order stiffness matrix, eigenvector, eigenvalue, and mass matrix, respectively.

Substituting Eq. (43) in Eq. (42) and collecting the similar order of terms, following zeroth, first and second order equations are obtained

$$[K^{(0)}] \{q^{(0)}\} = \lambda^{(0)} [M^{(0)}] \{q^{(0)}\} \quad (44)$$

$$[K^{(0)}] \{q^{(1)}\} + [K^{(1)}] \{q^{(0)}\} = \lambda^{(0)} [M^{(1)}] \{q^{(0)}\} + \lambda^{(0)} [M^{(0)}] \{q^{(1)}\} + \lambda^{(1)} [M^{(0)}] \{q^{(0)}\} \quad (45)$$

$$\{W_{ij}^{*II}\} = [K_0^{-1}] \quad (46)$$

$$\cdot \{F_{ij}^{*II} - [K_i^{*I}] \{W_j^{*I}\} - [K_j^{*I}] \{W_i^{*I}\} - [K_{ij}^{*II}] \{W_0\}\}$$

Obviously, Zeroth order Eq. (44) is the deterministic and gives the mean response. The first order Eq. (45) and second order Eq. (46) on other hand represents its random counterpart and solution of this equation provides the statistics of the vibration response, which can be solved using the probabilistic methods like perturbation technique, Monte Carlo simulation, Newman's expansion technique.

From these mean and covariance matrix of response vector, $\{\omega\}$ can be obtained as

$$\langle\{\omega\}\rangle \approx \{\omega_0\} + \frac{1}{2} \sum_{i=1}^N \sum_{j=1}^N \left\{ \omega_{ij}^{II} \right\} Cov [\alpha_i, \alpha_j] \quad (47)$$

$$Cov [\{\omega\}, \{\omega\}] \approx \sum_{i=1}^N \sum_{j=1}^N \left\{ \omega_i^{(1)} \right\} \cdot \left(\left\{ \omega_j^{(1)} \right\} \right)^T Cov [\alpha_i, \alpha_j] \quad (48)$$

After $Cov [\alpha_i, \alpha_j]$ is substituted in terms of correlation coefficients ρ_{ij} in Eq. (47), final expression for $Cov [\{\omega\}, \{\omega\}]$ is obtained as

$$Cov [\{\omega\}, \{\omega\}] = \sum_{i=1}^N \sum_{j=1}^N \left. \frac{\partial \{\omega\}}{\partial \alpha_i} \right|_{\alpha=0} \left(\rho_{ij} \sigma_{\alpha_i} \sigma_{\alpha_j} \right) \left. \frac{\partial \{\omega\}^T}{\partial \alpha_j} \right|_{\alpha=0} \quad (49)$$

where,

$$[\sigma_{\alpha}] = \begin{bmatrix} \sigma_{b1} & \dots & \dots & 0 \\ 0 & \sigma_{b2} & \dots & 0 \\ \dots & \dots & \dots & \dots \\ 0 & \dots & \dots & \sigma_{bm} \end{bmatrix} \quad (50)$$

$$\text{and } [\rho_{ij}] = \begin{bmatrix} 1 & \rho_{12} & \dots & \rho_{1m} \\ \rho_{21} & 1 & \dots & \rho_{2m} \\ \dots & \dots & \dots & \dots \\ \rho_{m1} & \rho_{m2} & \dots & 1 \end{bmatrix}$$

where $[\sigma_{\alpha}]$, $[\rho_{ij}]$ and m are the standard deviation (SD) of random variables, the correlation coefficient matrix and number of random variables, respectively. In the present analysis, the uncorrelated Gaussian random variable is taken into consideration. Therefore, covariance is equal to the variance.

The variance of the frequency of random variables b_i ($i = 1, 2, \dots, R$) and correlation coefficients can be expressed as

$$\text{var } \{\omega\} = \left(\frac{\partial \{\omega\}}{\partial b_i^R} \right) [\sigma_{\alpha}] [\rho_{ij}] [\sigma_{\alpha}] \left(\frac{\partial \{\omega\}}{\partial b_i^R} \right)^T \quad (51)$$

The standard deviation is taken as the square root of variance.

The second methodology known as Monte Carlo simulation (MCS) is based on the use of random variables and probabilistic statistics by direct use of a computer to investigate the problem. In the problem, a set of random numbers is generated first to represent the statistical uncertainties in the random structural parameters. These random numbers are then substituted into the deterministic response equation to obtain the set of random numbers which reflect the structural response [37, 38]. This

method is very simple and efficient when used with analytical response functions, but becomes computationally expensive when numerical methods are used to calculate the system response.

6 Results and discussion

The second-order statistics (mean, COV and PDF) of nonlinear fundamental frequency of CNTRC elastically supported beam by varying different foundation parameters, support conditions, slenderness ratios, amplitude ratios, and temperature increments, UD, FG-X and FG- λ distributed CNTRC with random system properties is investigated. A C^0 nonlinear finite element method based on direct iterative procedure combined with SOPT and MCS are used to evaluate the statistics of nonlinear fundamental frequency.

The accuracy of the present probabilistic approach is demonstrated by comparing the results with those available in the literatures and by employing MCS.

The basic random variables (b_i) are sequenced and defined as

$$\{b_i (i = 1, 2 \dots 16)\} = \{E_{11}^{cn}, V_{cn}, E_m, V_m, \nu_m, E_{22}^{cn}, G_{12}^{cn}, \nu_{cn}, \alpha_m, \alpha_{11}^{cn}, \alpha_{12}^{cn}, \rho_m, \rho_{cn}, k_1, k_2, k_3\}$$

where E_{11}^{cn} , V_{cn} , E_m , V_m , ν_m , E_{22}^{cn} , G_{12}^{cn} , ν_{cn} , α_m , α_{11}^{cn} , α_{12}^{cn} , ρ_m , ρ_{cn} , k_1 , k_2 and k_3 are the Young's modulus and volume fraction of carbon nanotube, Young's modulus and volume fraction of matrix, Poisson's ratios of matrix, thermal expansion coefficient and density of carbon nanotube and matrix, and linear Winkler, Shear and nonlinear Winkler foundation parameters, respectively.

In the present analysis, two combinations of displacement boundary conditions are used:

For simply supported (SS): $u = w = 0$

For clamped (CC): $u = w = \theta_x = \psi_x = 0$;

One edge is clamped and other is simply supported (CS): $u = w = \theta_x = \psi_x = 0$; at $x = 0$ and $u = w = 0$; at $x = a$

A stochastic finite element method (SFEM) based on FOPT, SOPT and MCS are used to evaluate the expected mean, coefficient of variation (COV) and PDF on dimensionless natural frequency of CNTRC elastically supported uncertain beam subjected to thermal loading.

The effective material properties of matrix (Polymethyl methacrylate) and the carbon nanotube (CNT) are assumed to be temperature dependent [15] which are given in Table 1.

Table 1: The effective material properties of matrix (Polymethyl methacrylate) and the carbon nanotube (CNT).

| Properties of matrix | | Properties of reinforcement (CNT) | | Efficiency parameter | | | |
|------------------------------------|---|--------------------------------------|----------|----------------------|----------|----------|----------|
| Young's modulus | (3.52-0.0034T) GPa | Young's modulus (E_{12}^{CN}) | 600 GPa | v_{cn}^* | η_1 | η_2 | η_3 |
| Thermal coefficient (α^m) | $45(1 + 0.0005\Delta T) \times 10^{-6}/K$ | Young's modulus (E_{22}^{CN}) | 10 GPa | 0.12 | 0.137 | 1.022 | 0.715 |
| Density (ρ^m) | 1150 kg/m ³ | Shear modulus (G_{12}^{CN}) | 17.2 GPa | 0.17 | 0.142 | 1.626 | 1.138 |
| Poisson's ratio | 0.34 | Poisson's ration (ν_{12}^{CN}) | 0.12 GPa | 0.28 | 0.141 | 1.585 | 1.109 |

Table 2: Convergence study of nonlinear fundamental frequency for UD distributed CNTRC beam with $V_{cn}^* = 0.28$, $W_{max}/h = 1.0$, and $a/h = 25$.

| No. of element | 16 | 20 | 24 | 30 | 40 | 50 | 60 |
|-------------------|---------|---------|----------|---------|---------|---------|---------|
| (ω_{NL}) | 23.2421 | 23.3206 | 23.38516 | 23.4427 | 23.4895 | 23.5256 | 23.5406 |

Table 3: Comparison of first three non-dimensional natural frequencies of UD and FG- Λ CNTRC beams at $T = 300$ K. The geometric parameter are taken to be $a/h = 12$, $h = 0.1$ m.

| ω_{NL} | Source | $V_{cn}^* = 0.12$ | | $V_{cn}^* = 0.17$ | | $V_{cn}^* = 0.28$ | |
|---------------|-----------------------|-------------------|---------------|-------------------|---------------|-------------------|---------------|
| | | UD | FG- Λ | UD | FG- Λ | UD | FG- Λ |
| 1 | Ke <i>et al.</i> [18] | 1.0431 | 0.9371 | 1.2947 | 1.2947 | 1.4927 | 1.3624 |
| | Present | 1.0829 | 0.9917 | 1.3104 | 1.2901 | 1.5186 | 1.3191 |
| 2 | Ke <i>et al.</i> [18] | 2.6791 | 2.5570 | 3.4048 | 3.4048 | 3.7156 | 3.6299 |
| | Present | 2.5167 | 2.5646 | 3.0700 | 2.9432 | 3.5150 | 3.5581 |
| 3 | Ke <i>et al.</i> [18] | 4.2850 | 4.9915 | 5.4923 | 5.4923 | 5.8808 | 5.8922 |
| | Present | 4.2816 | 5.0118 | 5.3186 | 5.7500 | 5.9443 | 6.1460 |

6.1 Convergence and validation study of second order statistics of transverse central deflation

The convergence study of mean dimensionless fundamental frequency by varying number of elements is examined by the direct iterative procedure is shown in Table 2. The considerable convergence in frequency parameter is shown as the number of element equal to 50. Therefore, in the present analysis, the total number of elements is taken as 50 until exclusively specified.

The accuracy and effectiveness of present deterministic finite element (FE) analysis are examined by comparison of first three non dimensionless natural frequencies with different volume fraction of CNTRC-UD distributed beams is shown in Table 3. Ke *et al.* [18] used first order shear deformation theory (FSDT) based semi analytical approach. It is evident from the table that both the results are in good agreement.

A comparison of present FE analysis of nonlinear to linear frequency ratios for an isotropic beam with various amplitude and slenderness ratios is shown in Table 4. The

dimensionless parameter for nonlinear frequency is taken as $\omega_0 = \omega_{NL} (a^2/h) \sqrt{12\rho/E}$ in the present study. The present C^0 finite element results are in good agreement with FSDT based semi-analytical approach investigated by Rao *et al.* [20].

The validation study of nonlinear to linear frequency ratio and different CNTRC distributed beam resting on Pasternak elastic foundation in thermal environment are shown in Table 5. The present results using C^0 FEM based on HSDT with von-Karman nonlinearity are in good agreement with Shen and Xiang [15] using HSDT based semi analytical approach.

6.2 Parametric study of second order statistics of nonlinear natural frequency

The effect of foundation parameters on nonlinear to linear frequency ratios of CNTRC beam with different CNT reinforcement distribution is shown in Fig. 3. The following dimensionless fundamental frequency (ω), foundation parameters (k_1, k_2 and k_3) and nonlinear to linear frequency

Table 4: Comparison of nonlinear to linear frequency ratio(R) of isotropic beam.

| W_{max}/h | $a/h = 25$ | | $a/h = 50$ | | $a/h = 100$ | |
|-------------|-----------------|---------|-----------------|---------|-----------------|---------|
| | Rao et al. [20] | Present | Rao et al. [20] | Present | Rao et al. [20] | Present |
| 0.0 | 1.0 | 1.0 | 1.0 | 1.0 | 1.0 | 1.0 |
| 0.2 | 1.0039 | 1.0041 | 1.0038 | 1.0037 | 1.0038 | 1.0036 |
| 0.4 | 1.0156 | 1.0162 | 1.0151 | 1.0147 | 1.0149 | 1.0142 |
| 0.6 | 1.0348 | 1.0355 | 1.0336 | 1.0323 | 1.0333 | 1.0313 |
| 0.8 | 1.0611 | 1.0609 | 1.0590 | 1.0558 | 1.0585 | 1.0542 |
| 1.0 | 1.0940 | 1.0991 | 1.0905 | 1.1437 | 1.0900 | 1.0868 |
| 2.0 | 1.3368 | 1.3491 | 1.3264 | 1.3210 | 1.3237 | 1.3124 |
| 3.0 | 1.6645 | 1.7004 | 1.6457 | 1.6473 | 1.6409 | 1.6313 |
| 4.0 | 2.0366 | 2.0781 | 2.0092 | 2.0060 | 2.0023 | 1.9848 |
| 5.0 | 2.4328 | 2.4674 | 2.4328 | 2.3794 | 2.3879 | 2.3544 |

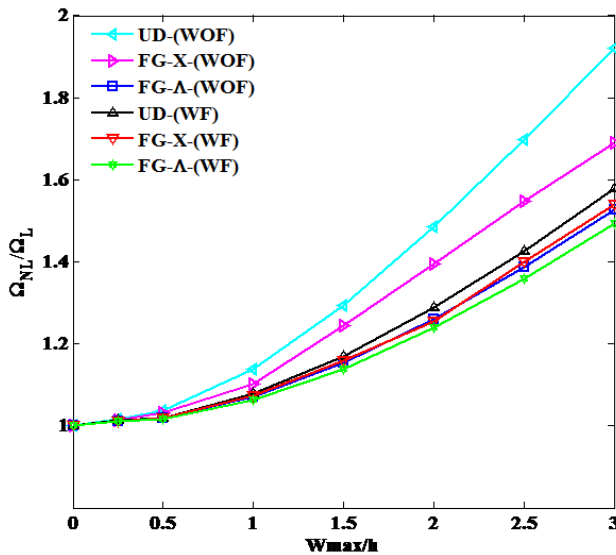


Figure 3: The effect of foundation stiffness on the amplitude-frequency curves of three types of CNTRC beam at $a/h = 50$, $V^*_{cn} = 0.28$, $T = 500$ K, $k_1 = 10^4$, $k_2 = 10^2$, $k_3 = 10^3$.

ratio are used in the present analysis are:

$$\bar{\omega} = \omega \left(a^2/h \right) \sqrt{\rho_0/E_0}, K_1 = k_1 \frac{E_0 h^3}{a^4},$$

$$K_2 = k_2 \frac{E_0 h^3}{a^2}, K_3 = k_3 \frac{E_0 h}{a^4}$$

The frequency ratio for UD, FG-X, and FG-A distributed beam increases with increase the amplitude ratios and foundation parameters. It is inferred from the figure that the frequency ratio is the maximum for UD type CNT reinforcement distribution in all the cases considered in the present study.

In fig. 4, the effect of volume fraction exponent on the vibration behavior of CNTRC beam with different CNT reinforcement distribution is depicted. The frequency ratio

for UD, FG-X, and FG-A distributed beam increases with increase the amplitude ratios, and volume fraction. This is due to the fact that, as the volume fraction increases, CNT reinforcement increases in the composite beam. In the consequence, stiffness increases, therefore natural frequency increases. Among the given different CNTRC distribution, The UD distributed CNTRC gives the highest frequency ratio for both the conditions *i.e.* with and without elastic foundation.

The effect of thermal environment on frequency ratios of CNTRC beam with different distribution is shown in Fig. 5. The frequency ratio for UD, FG-X, and FG-A distributed beam increases with an increase in the temperature and the amplitude ratios. Among the given different CNTRC distribution, the frequency ratio of UD distributed CNTRC is highest in all the cases considered in the study.

Table 6 shows the effects of individual random variables (b_i) on the dimensionless mean and COV of fundamental frequency of CNTRC elastically supported beam with UD and FG -X CNTRC distribution by assuming all system properties $\{b_i, (i = 1to16) = 0.10\}$ as uncorrelated random variables using SOPT and MCS under uniform pressure. Among the random system properties, beam is more sensitive in terms of the mean and COV of natural frequency to random change in E_{11}^{cn} , V_{cn} , V_m and K_2 . Tight controls of these random parameters are required for high reliability of CNTRC elastically supported beam. The statistics results using MCS are very close to SOPT results which show the efficacy of present approaches.

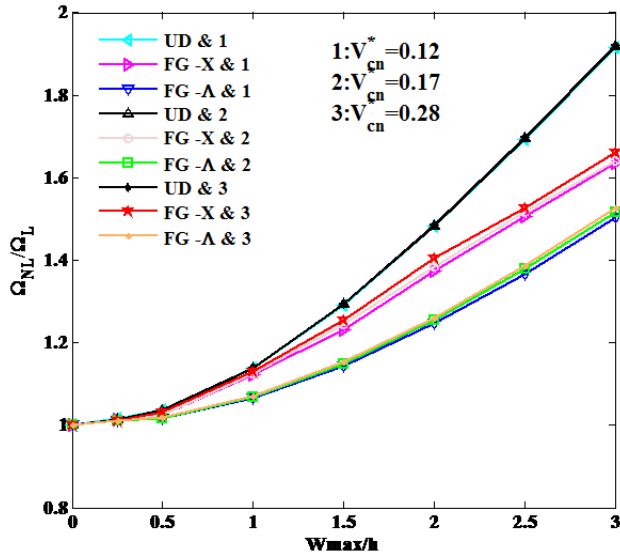
Table 7 shows the effects of different foundation parameters, CNTRC distribution and temperature increments with uncorrelated random system properties $\{b_i, (i = 1to16) = 0.10\}$ on the dimensionless mean and COV of nonlinear fundamental frequency of CNTRC beam using SOPT subjected to temperature dependent material prop-

Table 5: Validation table for nonlinear to linear frequency ratio ω_{NL}/ω_L for CNTRC beam resting on elastic foundation in thermal environment (The dimensionless frequency is defined as $\omega_0 = \omega_{NL} (a^2/h) \sqrt{\rho_0/E_0}$, $a/h = 25$, $V_{cn}^* = 0.28$).

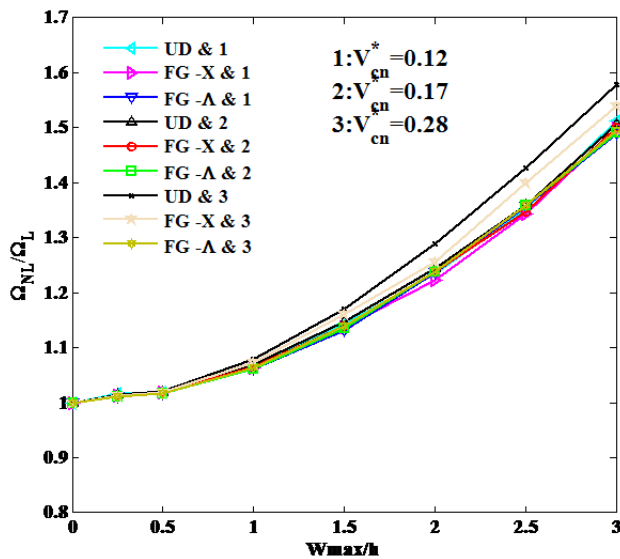
| k_1, k_2 | T(K) | CNTRC distribution | | ω_{0L} | W_{max}/h | |
|------------|------|--------------------|---------------------|---------------|-------------|--------|
| | | | | | 1.0 | 1.5 |
| (0,0) | 300 | UD | Present | 23.5698 | 1.1155 | 1.2465 |
| | | | Shen and Xiang [15] | 23.4774 | 1.1107 | 1.2352 |
| | | FG-A | Present | 19.5436 | 1.0389 | 1.0858 |
| | | | Shen and Xiang [15] | 19.9556 | 1.0398 | 1.0874 |
| | | FG-X | Present | 26.9164 | 1.0983 | 1.1913 |
| | | | Present | 27.1821 | 1.0837 | 1.1799 |
| | 500 | UD | Shen and Xiang [15] | 22.6109 | 1.1206 | 1.2569 |
| | | | Present | 22.4666 | 1.1178 | 1.2495 |
| | | FG-A | Shen and Xiang [15] | 19.3281 | 1.0390 | 1.0860 |
| | | | Present | 19.3026 | 1.0466 | 1.1021 |
| | | FG-X | Shen and Xiang [15] | 26.6578 | 1.0984 | 1.2113 |
| | | | Present | 25.6851 | 1.0913 | 1.1956 |
| (100,0) | 300 | UD | Present | 23.5701 | 1.1155 | 1.2465 |
| | | | Shen and Xiang [15] | 23.6439 | 1.1092 | 1.2322 |
| | | FG-A | Present | 19.5437 | 1.0389 | 1.0858 |
| | | | Shen and Xiang [15] | 20.1512 | 1.0412 | 1.0906 |
| | | FG-X | Present | 26.9165 | 1.0983 | 1.2113 |
| | | | Shen and Xiang [15] | 27.3261 | 1.0828 | 1.2322 |
| | 500 | UD | Present | 22.6113 | 1.1206 | 1.2569 |
| | | | Shen and Xiang [15] | 22.6405 | 1.1161 | 1.2461 |
| | | FG-A | Present | 19.3282 | 1.0390 | 1.0860 |
| | | | Shen and Xiang [15] | 20.3432 | 1.0529 | 1.1155 |
| | | FG-X | Present | 22.6579 | 1.0984 | 1.2113 |
| | | | Shen and Xiang [15] | 22.8237 | 1.1144 | 1.2427 |
| (100,10) | 300 | UD | Present | 24.3238 | 1.1066 | 1.2283 |
| | | | Shen and Xiang [15] | 23.8070 | 1.1078 | 1.2294 |
| | | FG-A | Present | 22.8503 | 1.0270 | 1.0602 |
| | | | Shen and Xiang [15] | 20.3424 | 1.0425 | 1.0934 |
| | | FG-X | Present | 27.6616 | 1.0917 | 1.1973 |
| | | | Shen and Xiang [15] | 27.4674 | 1.0520 | 1.1765 |
| | 500 | UD | Present | 23.3809 | 1.1106 | 1.2366 |
| | | | Shen and Xiang [15] | 22.8109 | 1.1144 | 1.2528 |
| | | FG-A | Present | 22.6656 | 1.0269 | 1.0599 |
| | | | Shen and Xiang [15] | 21.8757 | 1.0564 | 1.1230 |
| | | FG-X | Present | 27.4085 | 1.0916 | 1.1975 |
| | | | Shen and Xiang [15] | 25.9868 | 1.0892 | 1.1914 |

erties for $V_{cn}^* = 0.17$, $W_{max}/h = 1.0$. For the same foundation parameter, temperature increments and CNTRC distribution, as the slenderness ratio increases the mean fundamental frequency decreases and corresponding COV decreases. For the same slenderness ratio, temperature increments and CNTRC distribution, as the foundation parameters increase the mean fundamental frequency increases and corresponding COV decreases. It is because of foun-

dition parameters increase the stiffness of the plate. For the same slenderness ratio, foundation parameter and CNTRC distribution, as the temperature increases the mean fundamental frequency decreases and corresponding COV decreases. It is because of temperature increment lowers the stiffness of the beam. For the same slenderness ratio, foundation parameter and temperature increments, among the given CNTRC distributions, the mean funda-

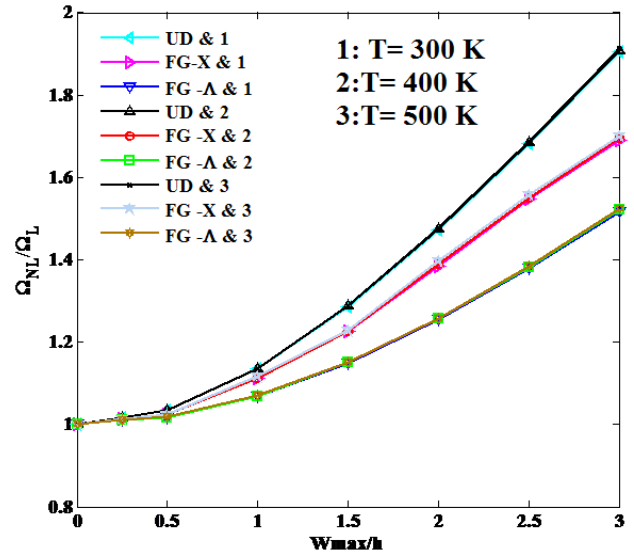


(a)

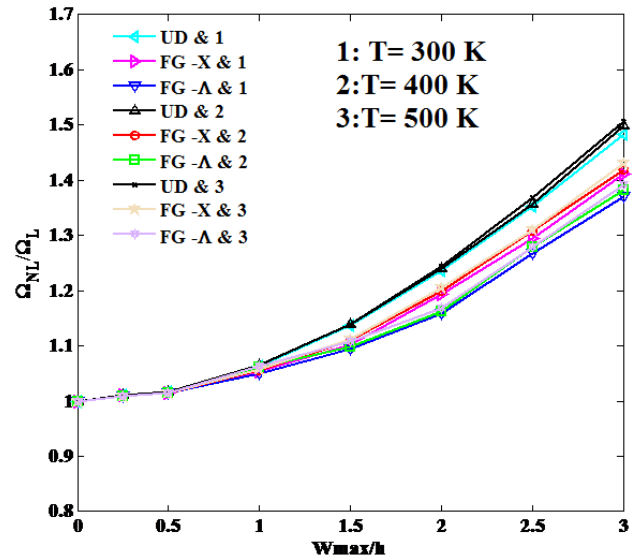


(b)

Figure 4: The effect of volume fraction on the amplitude –frequency curves of three types of CNTRC beam without elastically supported foundation (a) and with elastically supported foundation (b) at $a/h = 50$, $V^*_{cn} = 0.28$, $T = 500$ K, $k_1 = 10^4$, $k_2 = 10^2$, $k_3 = 10^3$.



(a)



(b)

Figure 5: The temperature variation on the amplitude –frequency curves of three types of CNTRC beam without elastically supported foundation (a) and with elastically supported foundation (b) at $a/h = 50$, $V^*_{cn} = 0.28$, $T = 500$ K, $k_1 = 10^4$, $k_2 = 10^2$, $k_3 = 10^3$.

mental frequency for FG- Λ is highest and correspond COV is low as compared to other distribution.

Table 8 shows the effects of support boundary conditions, foundation parameters and CNTRC distribution with uncorrelated random system properties $\{b_i, (i = 1 \text{ to } 16) = 0.1\}$ on the dimensionless mean and COV of fundamental frequency of CNTRC beam supported with (WF) and without (WOF) elastic foundation using SOPT and MCS. Among the different support conditions (SS, CC, and CS), dimensionless mean fundamental frequency of a clamped sup-

ported beam is highest while COV is highest for CS supported beam. It is because of less number of edge constraints present for CC supported beam. The dimensionless beam and COV of the fundamental frequency is lowered for elastically supported (WF) beam as compared to without supported (WOF) beam.

The effect of temperature increments and foundation parameters with all random system properties $\{b_i, (i = 1 \text{ to } 16) = 0.10\}$ on the PDF of nonlinear fundamental frequency of elastically supported beam by variation of UD,

Table 6: Effects of individual random variables (b_i) in case of UD and FG with random system properties $\{b_i, (i = 1, \dots, 16) = 0.1\}$ on the dimensionless mean and COV of nonlinear fundamental frequency of CNTRC beam with $T = 500K, V^*_{cn} = 0.17, W_{max}/h = 1.0, a/h = 25, k_1 = 10^4, k_2 = 10^2, k_3 = 10^3$.

| RV | CNRTC distribution | FOPT | | SOPT | | MCS | |
|-----------------------------|--------------------|---------|------------|---------|------------|---------|------------|
| | | Mean | COV | Mean | COV | Mean | COV |
| $b_1 = E^{cn}_{11}$ | UD | 18.9333 | 0.0230 | 19.0279 | 0.0229 | 18.8546 | 0.0231 |
| | FG-X | 29.4478 | 0.0264 | 29.7506 | 0.0262 | 29.8375 | 0.0281 |
| $b_2 = V_{cn}$ | UD | 18.9333 | 0.0127 | 18.9623 | 0.0127 | 18.8531 | 0.0126 |
| | FG-X | 29.4478 | 0.0140 | 29.5333 | 0.0140 | 29.8763 | 0.0192 |
| $b_3 = E_m$ | UD | 18.9333 | 0.0098 | 18.9505 | 0.0098 | 18.8587 | 0.0103 |
| | FG-X | 29.4478 | 0.0028 | 29.4513 | 0.0028 | 29.8635 | 0.0093 |
| $b_4 = V_m$ | UD | 18.9333 | 0.0475 | 19.3383 | 0.0465 | 18.9222 | 0.0481 |
| | FG-X | 29.4478 | 0.0344 | 29.9619 | 0.0338 | 29.9198 | 0.0355 |
| $b_5 = v_m$ | UD | 18.9333 | 0.0019 | 18.9339 | 0.0019 | 18.8698 | 0.0034 |
| | FG-X | 29.4478 | 2.5765e-05 | 29.4478 | 2.5765e-05 | 29.8483 | 0.0086 |
| $b_6 = E^{cn}_{22}$ | UD | 18.9333 | 5.6551e-15 | 18.9333 | 5.6551e-15 | 18.8657 | 5.6551e-15 |
| | FG-X | 29.4478 | 9.1105e-15 | 29.4478 | 9.1105e-15 | 30.0567 | 9.1105e-15 |
| $b_7 = G^{cn}_{12}$ | UD | 18.9333 | 5.9453e-05 | 18.9333 | 5.9453e-05 | 18.8654 | 6.8341e-05 |
| | FG-X | 29.4478 | 0.0101 | 29.4478 | 0.0101 | 29.8887 | 0.0101 |
| $b_8 = v_{cn}$ | UD | 18.9333 | 5.6551e-15 | 18.9333 | 5.6551e-15 | 18.8657 | 5.6551e-15 |
| | FG-X | 29.4478 | 9.1105e-15 | 29.4478 | 9.1105e-15 | 30.0567 | 9.1105e-15 |
| $b_9 = \alpha_m$ | UD | 18.9333 | 5.6551e-15 | 18.9333 | 5.6551e-15 | 18.8657 | 5.6551e-15 |
| | FG-X | 29.4478 | 9.1105e-15 | 29.4478 | 9.1105e-15 | 30.0567 | 9.1105e-15 |
| $B_{10} = \alpha^{cn}_{11}$ | UD | 18.9333 | 5.6551e-15 | 18.9333 | 5.6551e-15 | 18.8657 | 5.6551e-15 |
| | FG-X | 29.4478 | 9.1105e-15 | 29.4478 | 9.1105e-15 | 30.0567 | 9.1105e-15 |
| $B_{11} = \alpha^{cn}_{12}$ | UD | 18.9333 | 5.6551e-15 | 18.9333 | 5.6551e-15 | 18.8657 | 5.6551e-15 |
| | FG-X | 29.4478 | 9.1105e-15 | 29.4478 | 9.1105e-15 | 30.0567 | 9.1105e-15 |
| $B_{12} = \rho_m$ | UD | 18.9333 | 0.0096 | 18.9499 | 0.0096 | 18.8485 | 0.0105 |
| | FG-X | 29.4478 | 0.0129 | 29.5204 | 0.0129 | 29.8075 | 0.0160 |
| $B_{13} = \rho_{cn}$ | UD | 18.9333 | 0.0097 | 18.9501 | 0.0097 | 18.8685 | 0.0100 |
| | FG-X | 29.4478 | 0.0092 | 29.4846 | 0.0092 | 29.8605 | 0.0128 |
| $B_{14} = k_1$ | UD | 18.9333 | 6.3160e-05 | 18.9333 | 6.3160e-05 | 18.8655 | 7.8388e-05 |
| | FG-X | 29.4478 | 3.7192e-06 | 29.4478 | 3.7192e-06 | 29.8372 | 0.0092 |
| $B_{15} = k_2$ | UD | 18.9333 | 0.0170 | 18.9854 | 0.0170 | 18.8657 | 0.0170 |
| | FG-X | 29.4478 | 0.0112 | 29.5023 | 0.0112 | 29.8521 | 0.0139 |
| $B_{16} = k_3$ | UD | 18.9333 | 3.1680e-08 | 18.9333 | 3.1680e-08 | 18.8657 | 1.3690e-07 |
| | FG-X | 29.4478 | 0.0091 | 29.4840 | 0.0091 | 29.8332 | 0.0130 |

FG-X and FG- Λ is shown in Fig. 6. The temperature increment and foundation parameter makes the beam more sensitive in terms of the mean and variance of nonlinear fundamental frequency. As expected, the mean fundamental frequency for FG- Λ is highest and correspond COV is low as compared to other distribution.

The effect of COC on the PDF of nonlinear fundamental frequency and combined random variables $\{b_i, (i = 1 \text{ to } 16) = (0.05 - 0.20)\}$ on COV with and without foundation for UD, FG-X and FG- Λ is shown in Fig. 7. As the COC increases from 0.05-0.20, the dispersion in PDF increases

due to more deviation from the nonlinear fundamental frequency considering with and without foundation.

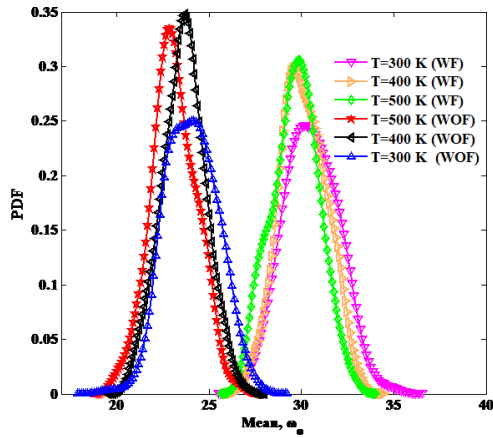
The of volume fraction on the PDF of nonlinear fundamental frequency and combined random variables $\{b_i, (i = 1 \text{ to } 16) = 0.10\}$ on COV with and without foundation for UD, FG-X and FG- Λ is shown in Fig. 8. As the volume fraction increases, the mean nonlinear fundamental frequency and dispersion in PDF increases. Considering the effect of foundation, the nonlinear fundamental frequency increases with increase in volume fraction and gives higher values as compared to without foundation.

Table 7: Effects of different combination of foundation stiffness parameters in case of UD and FG-X for random system properties $\{b_i, (i = 1 \text{ to } 16) = 0.10\}$ on the dimensionless mean and COV of nonlinear fundamental frequency of CNTRC beam, for $V_{cn}^* = 0.17$ $W_{max}/h = 1.0$.

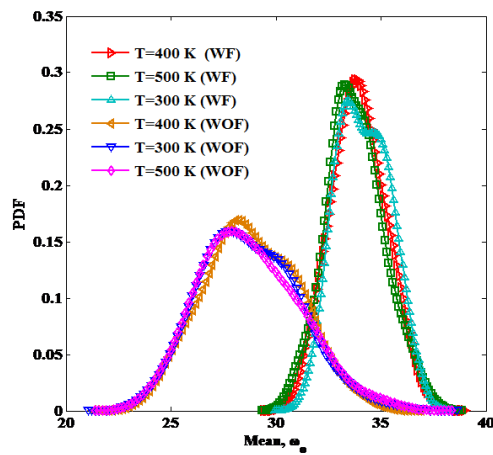
| a/h | Temp (K) | CNRTC distribution | k_1 | $k_3 = 0$ | | | | $k_3 = 1000$ | | | | |
|-------|----------|--------------------|---------|-----------|---------|-------------|---------|--------------|---------|-------------|---------|--------|
| | | | | $k_2 = 0$ | | $k_2 = 100$ | | $k_2 = 0$ | | $k_2 = 100$ | | |
| | | | | Mean | COV | Mean | COV | Mean | COV | Mean | COV | |
| 25 | 300 | UD | 0 | 21.1282 | 0.0641 | 28.7642 | 0.0488 | 21.1282 | 0.0641 | 28.7642 | 0.0488 | |
| | | FG-X | 0 | 26.0836 | 0.0619 | 31.1478 | 0.0459 | 28.4453 | 0.0547 | 35.3089 | 0.0423 | |
| | 500 | UD | 10^4 | 21.1429 | 0.0641 | 28.7779 | 0.0488 | 21.1426 | 0.0641 | 28.7779 | 0.0488 | |
| | | FG-X | 10^4 | 25.7683 | 0.0575 | 32.8217 | 0.0434 | 28.5711 | 0.0546 | 35.4315 | 0.0422 | |
| | 50 | 300 | UD | 0 | 20.2571 | 0.0652 | 28.0143 | 0.0490 | 20.2571 | 0.0652 | 28.0143 | 0.0490 |
| | | | FG-X | 0 | 25.5749 | 0.0614 | 30.8858 | 0.0470 | 27.9914 | 0.0540 | 35.4340 | 0.0438 |
| 500 | | UD | 10^4 | 20.2771 | 0.0651 | 28.0321 | 0.0490 | 20.2771 | 0.0651 | 28.0321 | 0.0490 | |
| | | FG-X | 10^4 | 23.2332 | 0.0651 | 30.9404 | 0.0481 | 28.3972 | 0.0551 | 35.3748 | 0.0427 | |
| 75 | | 300 | UD | 0 | 21.8811 | 0.0638 | 29.1946 | 0.0470 | 21.8811 | 0.0638 | 29.1946 | 0.0470 |
| | | | FG-X | 0 | 22.6672 | 0.0627 | 29.9728 | 0.0449 | 27.6890 | 0.0425 | 34.0471 | 0.0411 |
| | 500 | UD | 10^4 | 21.8846 | 0.0496 | 29.1985 | 0.0470 | 21.8846 | 0.0638 | 29.1985 | 0.0470 | |
| | | FG-X | 10^4 | 22.6684 | 0.0626 | 29.9741 | 0.0449 | 27.6900 | 0.0480 | 34.0483 | 0.0411 | |
| | 750 | UD | 0 | 21.3231 | 0.0651 | 28.7020 | 0.0473 | 21.3231 | 0.0651 | 28.7020 | 0.0473 | |
| | | FG-X | 0 | 22.3330 | 0.0648 | 29.7138 | 0.0458 | 27.4123 | 0.0491 | 33.8191 | 0.0418 | |
| 1000 | UD | 10^4 | 21.3279 | 0.0651 | 28.7070 | 0.0473 | 21.3279 | 0.0651 | 28.7070 | 0.0473 | | |
| | FG-X | 10^4 | 22.3342 | 0.0648 | 29.7151 | 0.0458 | 27.4131 | 0.0491 | 33.8202 | 0.0418 | | |

Table 8: Effects of boundary condition, UD , FG-X and FG- Λ considering with or without elastic foundation for random system properties $\{b_i, (i = 1 \text{ to } 16) = 0.10\}$ on the dimensionless mean and COV of nonlinear fundamental frequency of CNTRC beam under with $T = 300K$, $V_{cn}^* = 0.17$, $W_{max}/h = 1.0$, $a/h = 25$, $k_1 = 10^4$, $k_2 = 10^2$, $k_3 = 10^3$.

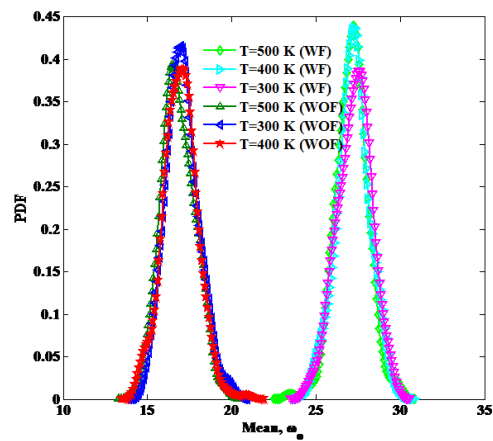
| BC | CNRTC distribution | Case | FOPT | | SOPT | | MCS | |
|------|--------------------|---------|---------|---------|---------|---------|---------|--------|
| | | | Mean | COV | Mean | COV | Mean | COV |
| SS | UD | WOF | 19.3853 | 0.0675 | 20.2420 | 0.0647 | 20.1373 | 0.0505 |
| | | WF | 27.7930 | 0.0555 | 28.9834 | 0.0532 | 27.7408 | 0.0403 |
| | FG- Λ | WOF | 14.1381 | 0.0650 | 14.5599 | 0.0631 | 14.1873 | 0.0597 |
| | | WF | 25.6541 | 0.0479 | 26.4106 | 0.0466 | 25.6230 | 0.0300 |
| CC | FG-X | WOF | 24.2473 | 0.0654 | 25.5030 | 0.0621 | 25.2607 | 0.5571 |
| | | WF | 34.3151 | 0.0472 | 35.6258 | 0.0454 | 34.1237 | 0.0357 |
| | UD | WOF | 35.2775 | 0.0670 | 36.0741 | 0.0621 | 35.1425 | 0.0511 |
| | | WF | 43.9747 | 0.0563 | 45.0409 | 0.0526 | 43.8369 | 0.0351 |
| CS | FG- Λ | WOF | 24.4737 | 0.0618 | 25.6181 | 0.0591 | 24.4079 | 0.0521 |
| | | WF | 35.8658 | 0.0489 | 37.4012 | 0.0469 | 35.8198 | 0.0342 |
| | FG-X | WOF | 38.0606 | 0.0659 | 40.2088 | 0.0609 | 39.9404 | 0.0640 |
| | | WF | 49.3540 | 0.0508 | 52.5004 | 0.0478 | 49.2881 | 0.0411 |
| CS | UD | WOF | 23.3401 | 0.0678 | 24.5927 | 0.0644 | 23.2424 | 0.0568 |
| | | WF | 39.8332 | 0.0580 | 42.5007 | 0.0543 | 39.7459 | 0.0369 |
| | FG- Λ | WOF | 15.9433 | 0.0573 | 16.3609 | 0.0559 | 15.2160 | 0.1291 |
| | | WF | 32.9787 | 0.0489 | 34.2807 | 0.0471 | 32.9357 | 0.0350 |
| FG-X | WOF | 16.7965 | 0.0663 | 17.4163 | 0.0639 | 17.2411 | 0.0762 | |
| | WF | 30.0985 | 0.0469 | 31.0965 | 0.0454 | 30.1685 | 0.0326 | |



(a)

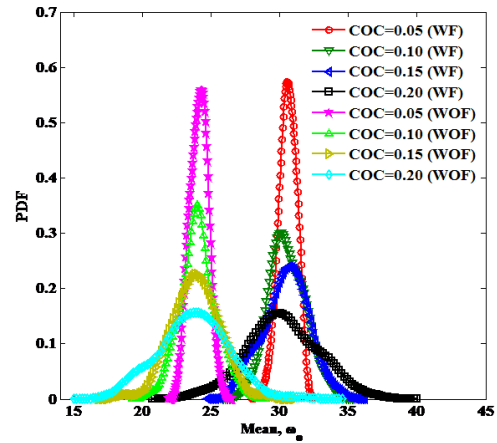


(b)

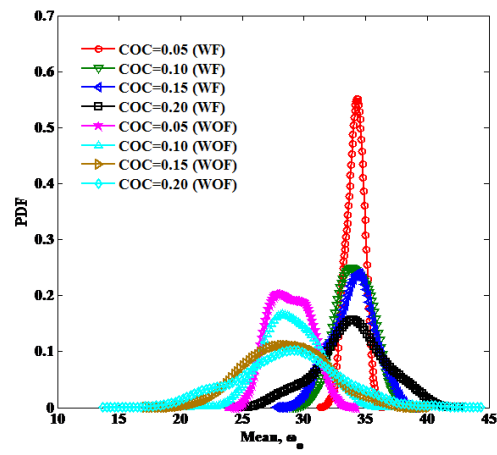


(c)

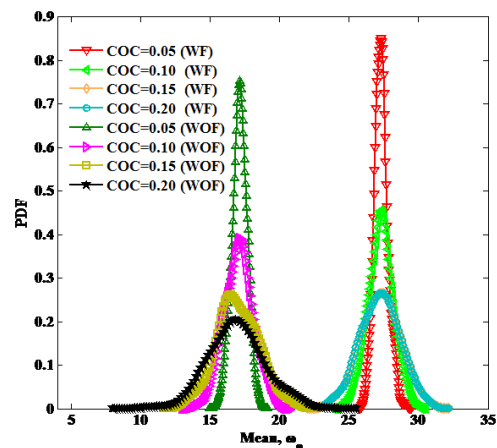
Figure 6: The effect of temperature variation on the PDF of nonlinear fundamental frequency of nonlinear elastically supported combined random variables $\{b_i, (i = 1 \text{ to } 16) = (0.10)\}$ with and without foundation for (a) UD and (b) FG-X and (c) FG-A distributed CNTRC beams at $a/h = 25$, $W_{\max}/h = 1$, $V_{cn}^* = 0.28$, $COC = 0.10$, $N = 10^4$.



(a)

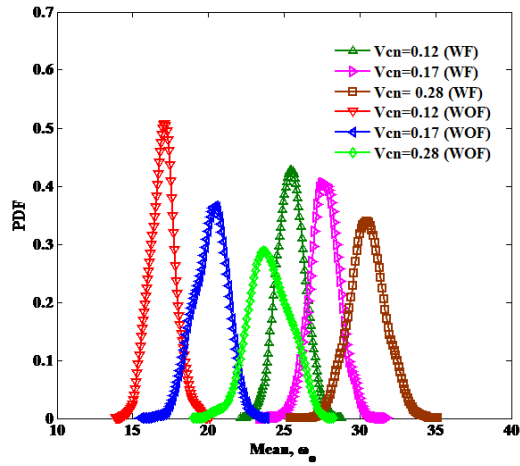


(b)

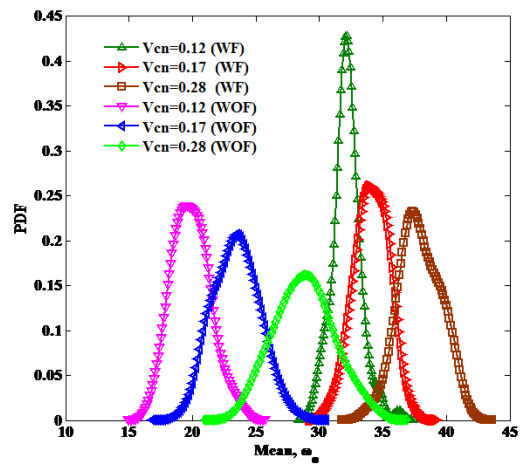


(c)

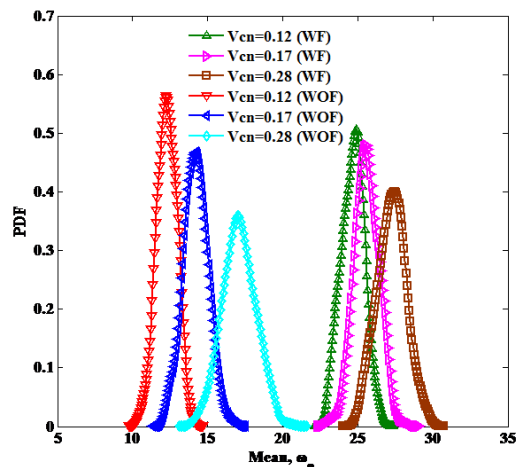
Figure 7: The effect of COC on the PDF of nonlinear fundamental frequency and combined random variables $\{b_i; (i = 1 \text{ to } 16) = (0.05 - 0.20)\}$ on COV with and without foundation for (a) UD and (b) FG-X and (c) FG-A distributed CNTRC beams at $a/h = 25$, $W_{\max}/h = 1$, $V_{cn}^* = 0.28$, $T = 300\text{K}$, $N = 10^4$.



(a)

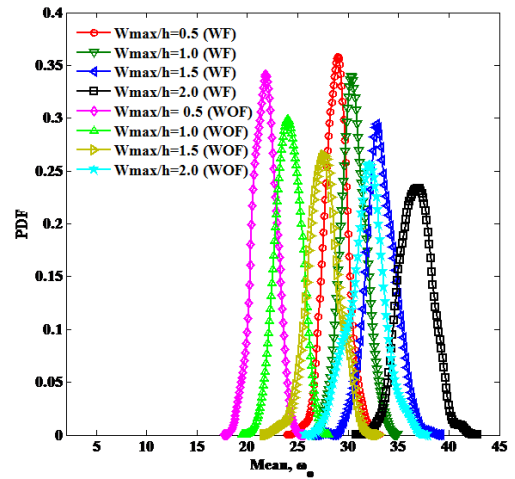


(b)

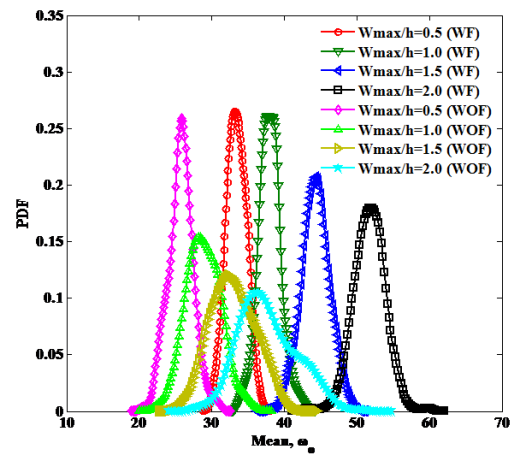


(c)

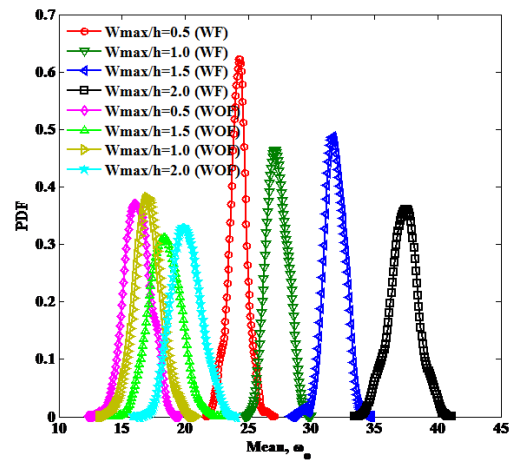
Figure 8: The effect of volume fraction on the PDF of nonlinear fundamental frequency and combined random variables $\{b_i, (i = 1 \text{ to } 16) = (0.10)\}$ on COV with and without foundation for (a) UD and (b) FG-X and (c) FG- Δ distributed CNTRC beams at $a/h = 25, W_{\max}/h = 1, V_{cn}^* = 0.28, COC = 0.10, N = 10^4$.



(a)

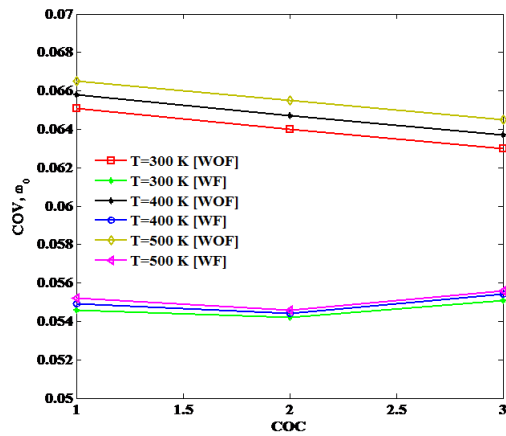


(b)

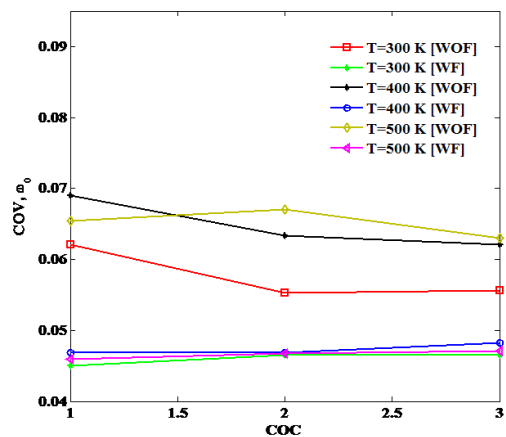


(c)

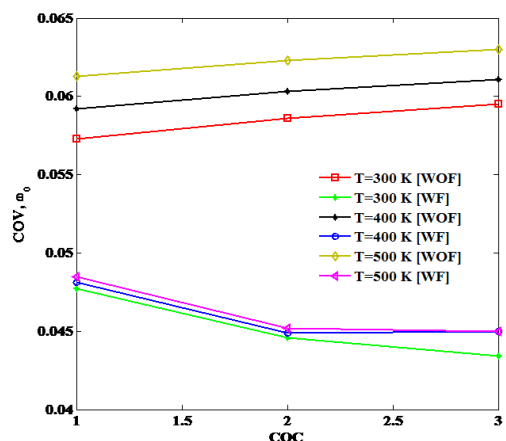
Figure 9: The effect of amplitude ratio on the PDF of nonlinear fundamental frequency and combined random variables $\{b_i, (i = 1 \text{ to } 16) = (0.10)\}$ on COV with and without foundation for (a) UD and (b) FG-X and (c) FG- Δ of CNTRC beams at $a/h = 25, V_{cn}^* = 0.28, T = 300 \text{ K}, COC = 0.10, N = 10^4$.



(a)



(b)



(c)

Figure 10: The effect of effect of temperatures and foundation parameters with combined random variables $\{b_i, (i = 1 \text{ to } 16) = (0.10)\}$ on dimensionless mean and COV of nonlinear fundamental frequency of simply supported CNTRC beam using SOPT in the case of (a) UD and (b) FG-X and (c) FG-A of CNTRC distributed beams at $a/h = 25, V_{cn}^* = 0.12, COC = 0.10, N = 10^4$.

The effect of amplitude ratio on the PDF of nonlinear fundamental frequency and combined random variables $\{b_i, (i = 1 \text{ to } 16) = 0.10\}$ on COV with and without foundation for UD, FG-X and FG-A is shown in Fig. 9. As the amplitude ratio increases, the nonlinear fundamental frequency and dispersion in PDF increases. Considering the effect of foundation, the nonlinear fundamental frequency increases with increase in amplitude ratio and gives higher values as compared to without foundation.

The effect of temperatures and foundation parameters with combined random variables $\{b_i, (i = 1 \text{ to } 16) = 0.10\}$ in the case of UD, FG-X and FG-A CNTRC distribution on the dimensionless mean and COV of nonlinear fundamental frequency of simply supported CNTRC beam using SOPT is shown in Fig. 10. As the temperature gradient increases, COV of nonlinear fundamental frequency increases. Considering the effect of foundation, the COV of nonlinear fundamental frequency increases with respect to temperature increment and gives lower values as compared to without foundation. It is because of temperature increments lowers the stiffness of the beam.

7 Conclusion

A direct iterative based C^0 finite element method combined with FOPT and SOPT and MCS though HSDT with von-Karman kinematic are used to evaluate the statistics of nonlinear fundamental frequency of elastically supported CNTRC beam in thermal environments. The results of FOPT and SOPT are validated by performing MCS. The beam is composed of UD, FG-X and FG-A distributed CNTRC. The mechanical properties of CNTRC are calculated on the basis of micromechanical based mechanics of material model. This work signifies the influences of random variables. The following conclusions are noted from the above study:

The results of dimensionless mean and COV of nonlinear fundamental frequency are in good agreements with SOPT and independent MCS approaches which shows the validity and efficacy of present approaches. The CNTRC elastically supported beam is more sensitive in terms of mean and COV of natural frequency by random change in system properties of E_{11}^{cn}, V_{cn}, V_m and k_2 . Tight control of these random parameters is required for high reliability of CNTRC elastically supported beam. For the given UD, FG-X and FG-A distributed CNTRC, the nonlinear frequency of FG-X is highest while COV of UD distribute CNTRC is highest. Extra care should be taken in the UD CNTRC distribution. For the given elastic foundations, the shear foun-

dition has a dominant effect in terms of the mean and COV of natural frequency. Proper control of shear foundation is required of the high reliability of the elastically supported CNTRC beam. As amplitude ratio increases, the mean and corresponding COV of fundamental frequency increases. Temperature increment makes the CNTRC beam more sensitive in terms COV. Therefore, for high temperature applications, strict control of temperature is highly desirable for reliability of structures. For reliability point of view, thick, clamp supported, high volume fraction of CNTRC beam should be preferred.

References

- [1] Iijima S., Helical microtubules of graphitic carbon, *Nature (London)*, 1991, 354, 56–8.
- [2] Thostenson E.T., Ren Z., Chou T.W., Advances in the science and technology of carbon nanotubes and their composites, a review, *Compos Sci Techno*, 2001, 61, 1899–912.
- [3] Lau K.T., Gu C., Gao G.H., Ling H.Y., Reid S.R., Stretching process of single- and multiwalled carbon nanotubes for nanocomposite applications. *Carbon*, 2004, 42, 426–8.
- [4] Wuite J., Adali S., Deflection and stress behavior of nanocomposite reinforced beams using a multiscale analysis, *Composites Structures*, 2005, 71, 388–96.
- [5] Vodenitcharova T., Zhang L.C., Bending and local buckling of a nanocomposite beam reinforced by a single-walled carbon nanotube, *International Journal of Solids and Structures*, 2006, 43, 3006–3024.
- [6] Hu N., Fukunaga H., Lu C., Kameyama M., Yan B., Prediction of elastic properties of carbon nanotube reinforced composites, *Proc Royal Soc A*, 2005, 461, 1685–710.
- [7] Han Y., Elliott J., Molecular dynamics simulations of the elastic properties of polymer/carbon nanotube composites, *Comput Mater Sci*, 2007, 39, 315–23.
- [8] Wan H., Delale F., Shen L., Effect of CNT length and CNT-matrix inter phase in carbon nanotube (CNT) reinforced composites, *Mech Res Commun*, 2005, 32, 481–9.
- [9] Shooshtari A., Rafiee M., Nonlinear forced vibration analysis of clamped functionally graded beams, *Acta Mech*, 2011, Doi: 10.1007/s00707-011-0491-1.
- [10] Yang J., Chen Y., Free vibration and buckling analysis of functionally graded beams with edge cracks, *Compos Struct*, 2008, 83, 48–60.
- [11] Ke L. L., Yang J., Kitipornchai S., Nonlinear free vibration of functionally graded carbon nanotube-reinforced composite beams, *Compos Struct*, 2010, 92, 676–83.
- [12] Kitipornchai S., Ke L-L., Yang J., Xiang Y., Nonlinear vibration of edge cracked functionally graded Timoshenko beams, *J Sound Vib*, 2009, 324, 962–982.
- [13] Sina S.A., Navazi H.M., Haddadpour H., An analytical method for free vibration analysis of functionally graded beams. *Mater Des*, 2009, 30, 741–747.
- [14] Aydogdu M., Vibration analysis of cross-ply laminated beams with general boundary conditions by Ritz method, *Int J Mech Sci*, 2005, 47, 1740–1755.
- [15] Shen H.S., Xiang Y., Nonlinear analysis of nanotube-reinforced composite beams resting on elastic foundations in thermal environments, *Engineering Structures*, 2013, 56, 698–708.
- [16] Boutaleb S., Zairi F., Mesbah A., Abdelaziz M. N., Gloaguen J.M., Boukharouba T., Lefebvre J.M., Micromechanics-based modelling of stiffness and yield stress for silica/polymer Nanocomposite, *International Journal of Solids and Structures*, 2009, 46, 1716–1726.
- [17] DeValve C., Pitchumani R., Analysis of vibration damping in a rotating composite beam with embedded carbon nanotubes, *Composite Structures*, 2014, 110, 289–296.
- [18] Ke L.L., Jieyang, Kitipornchai S., Dynamic Stability of Functionally Graded Carbon Nanotube-Reinforced Composite Beams *Mechanics of Advanced Materials and Structures*, 2013, 20.
- [19] Yas M.H., Samadi N., Free vibrations and buckling analysis of carbon nanotube-reinforced composite Timoshenko beams on elastic foundation, *International Journal of Pressure Vessels and Piping*, 2012, 98, 119–128.
- [20] Rao G.V., Varma R.R., Heuristic thermal post buckling and large-amplitude vibration formulations of beams. *AIAA J*, 2009, 47, 1977–80.
- [21] Mehdipour I., Barari A., Kimiaiefar A., Domairry G., Vibrational analysis of curved single-walled carbon nanotube on a Pasternak elastic foundation, *Advances in Engineering Software*, 2012, 48, 1–5.
- [22] Lee H. L., Chang W. J., Vibration analysis of a viscous-fluid-conveying single-walled carbon nanotube embedded in an elastic medium, *Physic Low-dimensional Systems and Nanostructures*, 2009, 41, 529–532.
- [23] Pradhan S. C., Murmu T., Differential Quadrature Method for Vibration Analysis of Beam on Winkler Foundation based on Nonlocal Elastic Theory. *J. Inst. Engg*, 2009, 89, 3–12.
- [24] Murmu T., Pradhan S. C., Thermo-mechanical Vibration of a Single-Walled Carbon Nanotube Embedded in an Elastic Medium based on Nonlocal Elasticity Theory, *Comput. Mater. Sci*, 2009, 46, 854–869.
- [25] Yoon J., Ru C.Q., Mioduchowski A., Vibration of an embedded multiwall carbon nanotube, *Comput. Sci. Technol*, 2003, 63, 1533–1542.
- [26] Timoshenko S.P., Young D.H., Weaver W., *Vibration Problems in Engineering*, New York, Wiley, 1974.
- [27] Chaudhari V. K., Lal A., Nonlinear free vibration analysis of elastically supported nanotube reinforced composite beam in thermal environment, *Procedia Engineering*, 2016, 144, 928 – 935.
- [28] Fantuzzi N., Tornabene F., Baccocchi M., Dimitri R., Free vibration analysis of arbitrarily shaped functionally graded Carbon Nanotube-reinforced plates, *Composites Part B*, 2016, doi: 10.1016/j.compositesb.2016.09.021.
- [29] Tornabene F., Fantuzzi N., Baccocchi M., Linear static response of nanocomposite plates and shells reinforced by agglomerated carbon nanotubes, *Composites Part B* 2016, 1–28.
- [30] Shegokar N. L., Lal A., Stochastic finite element nonlinear free vibration analysis of piezoelectric functionally graded materials beam subjected to thermo-piezoelectric loadings with material uncertainties, *Meccanica*, 2013, DOI 10.1007/s11017-9852-2.
- [31] Vanmarcke E., Grigoriu M., Stochastic finite element analysis of simple beams, *J Eng Mech*, 1983, 109 (5), 1203–1214.
- [32] Kaminski M., Stochastic second-order perturbation approach to the stress-based finite element method, *Int J Solids Struct*,

- 2001, 38, 3831–3852.
- [33] Locke J.E., Finite element large deflection random response of thermally buckled plates. *J Sound Vib*, 1993, 160, 301–312.
- [34] Onkar A.K., Yadav D., Forced nonlinear vibration of laminated composite plates with random material properties, *Compos Struct*, 2005, 70, 334–342.
- [35] Kitipornchai S., Yang J., Liew K. M., Random vibration of functionally graded laminates in thermal environments, *Comput Methods Appl Mech Eng*, 2006, 195, 1075–1095.
- [36] Shaker A., Abdelrahman W., Tawfik M., Sadek E., Stochastic finite element analysis of the free vibration of functionally graded material plates, *Comput Mech*, 2008, 41, 707–714.
- [37] Lal A., Singh B.N., Stochastic nonlinear free vibration response of laminated composite plates resting on elastic foundation in thermal environments, *Comput Mech*, 2009, 44, 15–29.
- [38] Lal A., Singh B.N., Kumar R., Natural frequency of laminated composite plate resting on an elastic foundation with uncertain system properties, *Struct Eng Mech*, 2007, 27, 199–222.
- [39] Jagtap K. R., Lal A., Singh B.N., Stochastic nonlinear free vibration analysis of elastically supported functionally graded materials plate with system randomness in thermal environment, *Compos Struct*, 2011, 93, 3185–3199.